F. FUNDAMENTAL INTERACTIONS AND OTHER TOPICS

The nucleus remains one of nature's classic laboratories for studying both the strong and weak interactions, and is ideal for studying the quantum mechanics of small, but finite, systems. Some of the ideas and techniques developed for understanding nuclei have found new applications in understanding the physics of clusters of atoms and in assemblies of atoms constrained by traps. Similarly, some of the accelerators and detection techniques of nuclear physics have been used for ultra-sensitive trace element measurement, in Accelerator Mass Spectrometry. We continue to be interested in finding new avenues where our knowledge and equipment can be applied to important projects.

f.1. Specific Heat and Phase Transition in Confined Ionic Systems (J. P. Schiffer)

The study of discrete charges confined in space, such as ions in an ion trap, shows ordered quasi-crystalline structuring at low temperatures. In isotropic confinement the ions form a spherical cloud whose radius is determined by the strength of the confining force and the number of ions, and within, the ions arrange themselves to be as equally spaced as possible. For relatively few ions ($\lesssim$ 100,000) this results in the ions forming into concentric shells, and within each shell a pattern of equilateral triangles.

For an infinite system of ions (a one-component plasma, or OCP) the ordering takes a body-centered cubic form, and the phase transition from liquid to solid takes place at a temperature corresponding to

$$\Gamma = \frac{q^2 / a_{WS}}{kT} \cong 173,$$

or

$$T \cong \frac{q^2 / a_{WS}}{173\,k}$$

where a_{WS} is the Wigner-Seitz radius and k is Boltzmann's constant. The form of ordering in the finite confined systems is governed by the boundary conditions that form a spherical (and curved) surface, and it is not simply related to the body-centered cubic form for infinite matter.

The energy associated with this phase transition (or latent heat), and the specific heat, or the amount of energy it takes to accomplish a given change in temperature, were studied. Earlier work investigated the behavior of the infinite OCP in simulations — though these quantities had apparently not been extracted explicitly. In the finite confined systems, it appeared from simulations that the formation of shells was a more gradual process, though it seemed to occur roughly at the above temperature.

To investigate the specific heat behavior in these finite systems, simulations were carried out on 1000 and 10,000 ion systems using the method of Molecular Dynamics, where the Newtonian trajectories of all particles are followed explicitly in small time steps. The specific heat is then defined as the ratio in the change in kinetic energy (temperature) of the system divided by the corresponding change in total energy.

The simulations were carried out starting from a cold system that was prepared by slowly cooling and annealing the particles confined under a constant confining harmonic force,

$$F = -Kr$$

while requiring the temperature to be low (0.0003 in the above units). This system was heated in increments by adding fixed amounts of energy (scaling up the thermal velocity distribution). The simulation then was allowed to coast for a large number of time steps in the simulations. The natural unit of time in such a system is the period corresponding to the plasma frequency — and this coasting time was typically 2000 time steps, or about 50 plasma periods. The average kinetic energy and total energy were then obtained by averaging the values for the next 8000 time steps (about 200 plasma

periods). This then was repeated a number of times to obtain values of specific heat over the temperature range that covered roughly two orders of magnitude, centered on the transition temperature. Different methods were also tried, for instance, using new velocity distributions for each temperature, or adding heat repeatedly until a predetermined temperature was reached and then observing the equilibrium state.

The ratios of the changes in total energy to those in the kinetic energy are shown in Fig. I-75, indicating an increase in the ratio at about the temperature of the expected phase transition. This transition is shown in more detail in Fig. I-76 in terms of the specific heat. It appears that the behavior of the confined ions is very similar to that of the infinite medium. The difference in the transition temperature was not well determined in the simulations and different simulations gave somewhat different results. This is being investigated further.

Finally, the level of ordering associated with this transition was also investigated in terms of the correlation function g(r). The first peak in the correlation function decreases, and then disappears as the temperature increases over the transition region — going over to a smooth behavior characteristic of a liquid or gas. The height of this first peak in the correlation function, divided by the height of the first minimum following it, is plotted in Fig. I-77. It is clear that the peak in specific heat is associated with the phase transition, and that this transition appears to occur more slowly than in the infinite system, but at very nearly the same temperature.

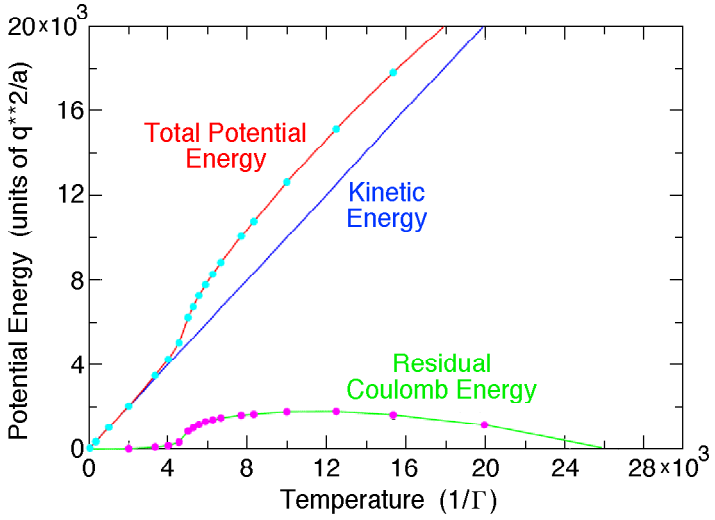

Fig. I-75. The potential energy per ion of a system of 10,000 ions is plotted in units of the Coulomb energy between two adjacent particles. The zero of the potential energy, a combination of the Coulomb energy and that in the focusing field, is chosen such that it is zero at zero temperature. The potential energy increases linearly with temperature at first, but then shows an anomaly that is associated with the system becoming disordered.

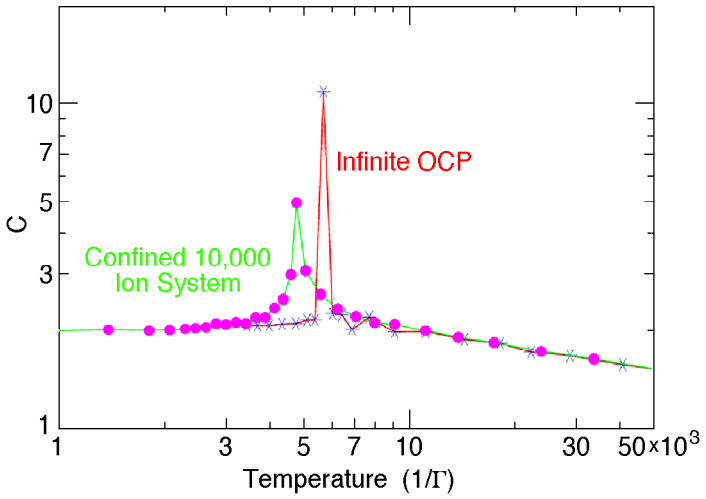

Fig. I-76. The specific heat is plotted for the system of 10,000 ions and compared to that from the literature for infinite coulombic matter. The difference in the transition temperature is probably not significant, and depends on the detailed conditions of the simulation.

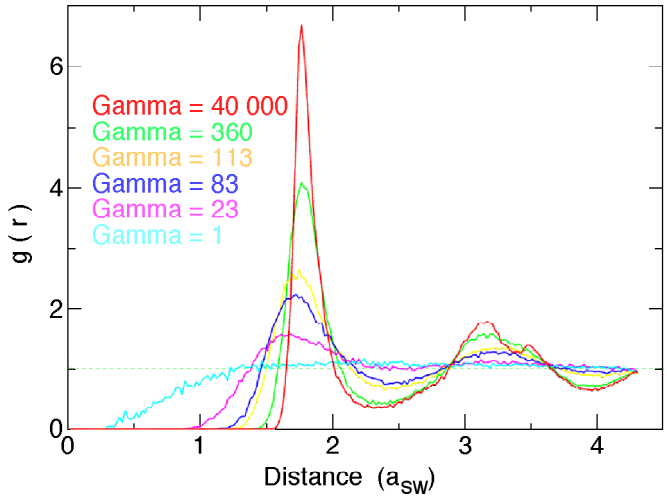

Fig. I-77. The correlation functions g(r) are plotted as a function of distance in units of the Wigner-Seitz radius a_{WS} for various values of the temperature in the upper part of the figure. The quantity Γ is the reciprocal temperature in units of q^2/a_{WS}. The lower part of the figure shows the ratio of the maximum in the correlation function to the subsequent minimum, as a function of the parameter Γ. The point of the phase transition for an infinite plasma at $\Gamma = 173$ is indicated.

f.2. **Comparison of Classical Configurations in Two-Dimensional Confinement with Those of the Quantum-Mechanical System of Quantum Dots** (John Schiffer and David Dean*)

The behavior of quantum dots, magnetic flux lines trapped and confined in magnetic fields, shows simple patterns that were reproduced by fully quantum-mechanical Hartree-Fock calculations. The classical system of charges confined to two dimensions, and within the two dimensions by a harmonic potential around the origin, was explored using the Molecular Dynamic simulations that were used to study ordering phenomena in three-dimensional plasmas.

In the simulations, the particles were started with random velocities in two dimensions and then allowed to move, following Newtonian dynamics, in small time steps. The velocities of the particles were slowly reduced until there was no further motion possible. This procedure was repeated up to 100 times with different random initial coordinates and velocities, in order to insure that the minimum reached was not a false (isomeric) minimum. When more than one configuration appeared, the one with the lowest energy was chosen.

The patterns seen in these classical simulations are remarkably similar to the quantum-dot calculations seen in Fig. I-78 for up to 16 particles.

For instance, in both cases, five particles form in a pentagon in each system while 6 particles form a pentagon with one in the center,

6 to 8 particles have 1 inside
9 and 10 particles have 2 inside
11 and 12 have 3
13 and 14 have 4
15 has 5
16 has 6

The only noticeable difference is for 10 particles, where the 2 inner ones line up in a row with two outer ones in the classical simulations, while they do not do this for the quantum dots. The two configurations are close in energy but the lower energy one was picked in each case. Since the quantum dot calculation involves interactions quite different from the classical Coulomb force with, for instance, exchange terms in the interaction, the similarities are rather surprising.

*Oak Ridge National Laboratory

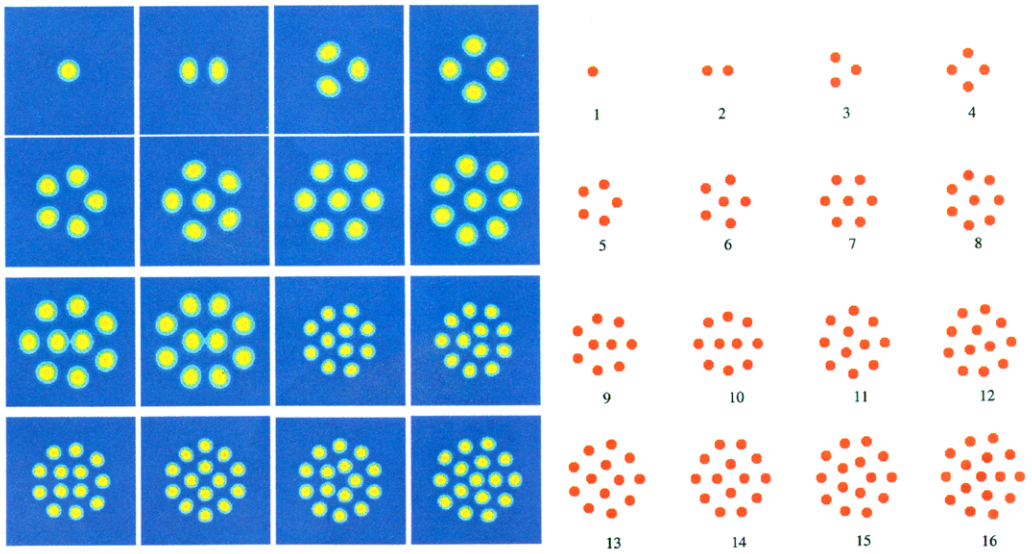

Fig. I-78. The pattern of configurations for quantum dots (left) and for classical simulations of charges confined in two dimensions by a harmonic potential (right) are compared.

f.3. A Proposed Method for Measuring the Electric Dipole Moment of the Neutron by a Large Improvement of the Shull Method

(T. W. Dombeck,* M. Peshkin, and G. R. Ringo)

Experiments to measure the electric dipole moment (EDM) of the neutron by subjecting neutrons to an external magnetic field and observing their spin precession currently find that the EDM vanishes with an uncertainty of 1×10^{-25} e-cm, that sensitivity being limited by systematic errors. We are doing feasibility studies for a different kind of experiment which will have completely different, and possibly smaller, systematic errors. In this new experiment, polarized neutrons will undergo several thousand Bragg reflections in a slot cut in a perfect silicon crystal. At each reflection, their polarization will be rotated by the action of the crystalline electric field on the neutron's EDM, and the accumulated rotation will be measured. The hoped-for improvement in sensitivity relies upon the great magnitude of the crystalline electric field, which are four orders of magnitude stronger than external electric fields that can be achieved practically at the Ramsey experiments. This method should be simpler and less expensive than the interferometric measurement that we proposed in 1997[1], but possibly somewhat less sensitive.

An experiment by Shull and Nathans in which neutrons were transmitted through a crystal confirmed the effective crystalline field by observing the stronger interaction with the neutron's magnetic dipole moment (MDM). The moving MDM interacts with the electric field as an effective EDM equal to (v/c) times the MDM. Our experiment will amplify the affect of the EDM interaction by having thousands of bounces from the crystal while the moving MDM effect will be suppressed by suitable arrangement in magnetic guide fields.

Preliminary experiments at the Missouri reactor encouraged us to try an experiment with greater sensitivity to the Bragg-angle reflectivity of the perfect silicon crystal, which is required to allow several thousand Bragg reflections without significant loss of neutrons. Such an experiment was done at the Missouri reaction in 2000. We were able to get an average reflectivity of 0.99998 for each of 380 Bragg reflections. We plan a test of Schwinger scattering which should lead to a full-scale design that we hope to try on a higher flux source, possible HIFR at Oak Ridge National Laboratory.

*Fermi National Accelerator Laboratory

1M. S. Freedman, G. R. Ringo, and T. W. Dombeck, Nucl. Instrum. Methods **A396**, 181 (1997).

f.4. The Quest for a Detection Method of Natural ^{39}Ar

(Ph. Collon, I. Ahmad, J. Caggiano, C. L. Jiang, A. Heinz, D. Henderson, R. C. Pardo, K. E. Rehm, R. Vondrasek, W. S. Broecker,* L. DeWayne Cecil,† Y. El Masri,‡ W. Kutschera,§ P. Leleux,‡ M. Paul,¶ P. Schlosser,* R. H. Scott, and W. M. Smethie, Jr.*)

This program is devoted to developing a viable method for the measurement of cosmogenic ^{39}Ar at or below natural levels (^{39}Ar/Ar = 8.2×10^{-16})with Accelerator Mass Spectrometry (AMS) at ATLAS. A half-life of 268 years and its conservative geochemical behavior make ^{39}Ar one of the most sought after dating and tracing tools for oceanography and hydrology. Initial experiments in 1992 at the ATLAS facility resulted in a clear detection of a ^{39}Ar signal at the natural level. Though, at the time, the overall low efficiency made any attempt at measuring natural samples impractical, this first experiment laid down a solid base for future developments. Several improvements in the ECR source, the development of a gas handling system that enables us to inject small (> 4 cm_3 STP) argon gas samples into the ECR source and a new detector with larger vertical aperture, for used in the gas filled Enge split-pole spectrograph, encouraged us to continue to develop this method. The goal of the program is to demonstrate the feasibility of measuring ^{39}Ar/^{40}Ar

ratios in argon samples for practical applications in oceanography and groundwater hydrology.

The successful run in February of 2001 at ATLAS showed that enriched (^{39}Ar/Ar = 4.6 × 10$^{-13,}$ see Fig. I-79), natural (^{39}Ar/Ar = 8.2 × 10^{-16}) and below natural ^{39}Ar levels (^{39}Ar/Ar = 2.2 × 10$^{-16,}$ see Fig. I-80) can be measured for the first time by AMS. The ^{39}K background which was the major obstacle to these measurements was found to be controllable at the ECR II ion source as well as the detector setup level. In addition to this, it was possible to measure the ^{39}Ar/Ar ratio in 3 ocean water samples collected during the SAVE (South Atlantic Ventilation Experiment) sampling trip. These gas samples where extracted from 20 liter of deep ocean water (< 4000 m depth) taken off the coast of Brazil. The results from these samples where found to be within the expected ranges determined by J. Rodriguez and H. H. Loosli from the University of Bern using Low Level Counting on argon samples from the same region and depth of ocean[1].

At present the natural level ^{39}Ar samples yield ~8 counts per hour. Expected improvements in the overall efficiency (e.g. ion source output, further reduction of the potassium as well as the detection efficiency) should bring an overall factor of ~10 in the coming runs. Moreover we were able to determine that the ionization efficiency of the gas sample into the ^{39}Ar^{8+} charge state is as high as 2 to 3%, leading to a very low sample gas consumption rate.

---

*Lamont-Doherty Earth Observatory of Columbia University, Palisades, NY, †US Geological Survey, Idaho Falls, ID, ‡Catholic University of Louvain, Belgium, §University of Wien, Austria, ¶Hebrew University of Jerusalem, Israel

1J. Rodriguez, *Beitraege zur Verteilung von ^{39}Ar im Atlantic*, Thesis presented to the Philosophisch-naturwissenschaftlichen Fakultaet of the University of Bern, Switzerland, 1993.

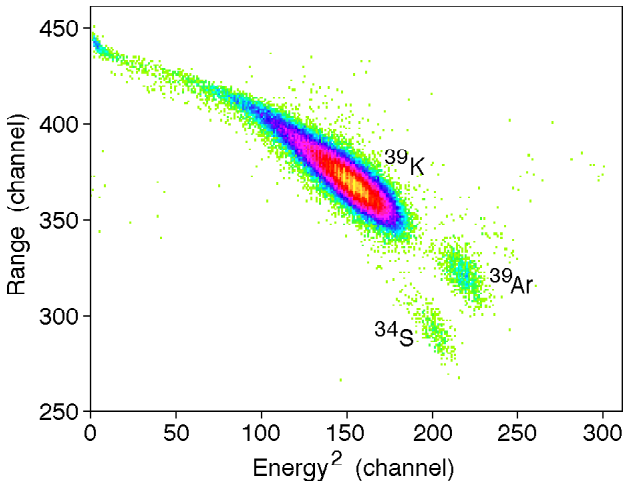

Fig. I-79. Measurement of an enriched ^{39}Ar (^{39}Ar/Ar = 4.6 × 10^{-13}) sample used to determine the position of the ^{39}Ar peak measured in the gas-filled split pole spectrograph. Run time 26 min; 830 counts.

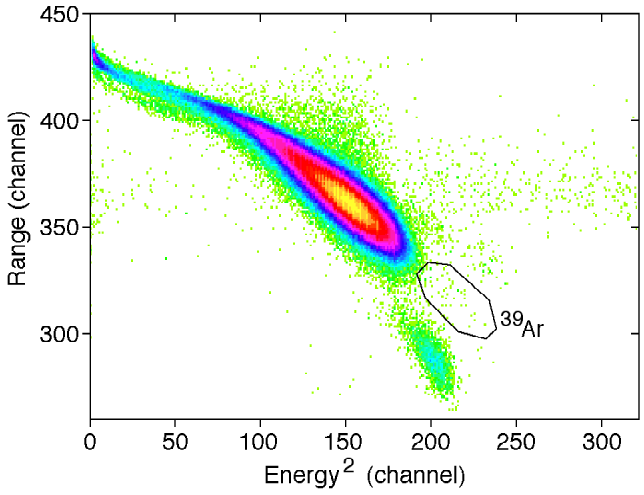

Fig. I-80. Measurement of an ocean water sample LDEO-191 (^{39}Ar below natural level; $^{39}Ar/Ar = 2.2 \times 10^{-16}$). Run time 10 hours 35 min.

f.5. Ultra-Sensitive Detection of ^{244}Pu by Accelerator Mass Spectrometry (I. Ahmad, M. Paul,* D. Berkovits,† and A. Valenta*‡)

We are pursuing a program of ultra-high sensitivity detection of actinide elements by Accelerator Mass Spectrometry (AMS). The rare isotope ^{236}U ($T_{1/2}$ = 23.4 Myr) was recently successfully detected in uranium minerals and standards.[1,2] The case of ^{244}Pu, the longest-lived ($T_{1/2}$ = 80 My) actinide after ^{232}Th and ^{238}U, is particularly interesting. Its presence in early-solar material was positively inferred from isotopic anomalies of Xe trapped inside meteorites (Ref. 3 and references therein) which were shown to originate in ^{244}Pu spontaneous fission. The ^{244}Pu abundance relative to ^{238}U at the time of the solar system formation was established from these isotopic anomalies to be 0.007 while the ratio of their production estimated from *r*-process models (and somewhat uncertain within a factor of two) is 0.7 (Ref. 4). The ratio between these relative abundances possibly originates in a time delay between synthesis and condensation. This time delay is, however, different from that estimated from other short-lived nuclides such as ^{26}Al ($T_{1/2}$ = 0.72 My) and ^{41}Ca (0.10 My) whose presence in early-solar material was also inferred[5] from abundance anomalies (^{26}Mg, ^{41}K, respectively). Different mechanisms and sites of synthesis are therefore suggested. The presence of ^{244}Pu (and other *r*-process short-lived nuclides) in the interstellar material has not been observed at this point. Surprisingly, evidence for presence of live ^{244}Pu in a rare-earth mineral on Earth was reported[6] but never confirmed since. A hypothesis that this nuclide could originate from extraterrestrial material deposited on Earth (and later abducted into the mineral) was considered.[6]

The detection of ^{244}Pu by alpha spectrometry is limited by the long half-life, making atom counting by mass spectrometry more efficient, favored also by the absence of long-lived isobaric 244 nuclides. Accelerator Mass Spectrometry (AMS) is particularly discriminative owing to total elimination of molecular interferences. In order to estimate the efficiency and sensitivity of an AMS determination of ^{244}Pu, we prepared samples containing 4×10^{10} ^{244}Pu atoms in a Fe_2O_3 matrix and measured the isotopic distribution by AMS. The samples were made from an iron nitrate solution (2.4 mg Fe^{3+}) spiked with 40 µL of a Pu solution enriched in ^{244}Pu (0.37 ng/mL). Pu was coprecipitated with iron hydroxide and the latter ignited to Fe_2O_3, then pressed in a 1-mm diameter hole of the cathode holder. The AMS measurements were performed at the 14UD Pelletron Koffler Accelerator Laboratory (Israel). PuO^- ions were extracted from a high-intensity Cs sputter ion source. After foil stripping in the tandem terminal, $^{A}Pu^{11+}$ ions (A = 240,242,243,244) were successively analyzed and counted in a TOF-ionization chamber telescope. The measured isotopic distribution (Fig. I-81) is in good agreement with the calibrated values. From the count rate of the measurements, it is established that the sensitivity limit of the detection is ~1 × 10^6 ^{244}Pu atoms.

*Hebrew University, Jerusalem, Israel, †Soreq NRC, Yavne, Israel, ‡University of Vienna, Austria

1M. Paul *et al*., Nucl. Instrum. Methods in Phys. Res. **B172**, 688 (2000).
2D. Berkovits *et al*., Nucl. Instrum. Methods in Phys. Res. **B172**, 372 (2000).
3G. J. Wasserburg, in *Protostars and Planets II*, ed. D. C. Back and M. Matthews (Tucson, U. Arizona Press), 703, (1985).
4B. S. Meyer and D. D. Clayton, Space Sci. Rev. **92**, 133 (2000).
5T. Lee, D. A. Papanastassiou, and G. J. Wasserburg, Geophys. Res. Lett. **3**, 109 (1976).
6D. C. Hoffman, F. O. Lawrence, J. L. Mewherter, and F. M. Rourke, Nature **234**, 132 (1971).

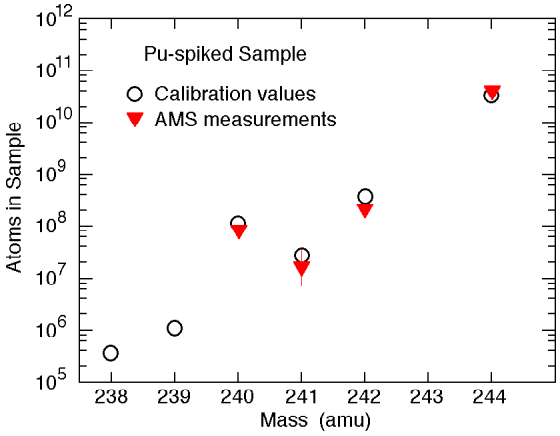

Fig. I-81. Mass distribution of an enriched ^{244}Pu sample measured by AMS.